

Two-dimensional χ^2 solitons generated by the downconversion of Airy waves

Thawatchai Mayteevarunyoo

*Department of Telecommunication Engineering,
Mahanakorn University of Technology, Bangkok 10530*

Boris A. Malomed

*Department of Physical Electronics,
School of Electrical Engineering, Faculty of Engineering,
Tel Aviv University, Tel Aviv 69978, Israel*

Abstract

Conversion of truncated Airy waves (AWs) carried by the second-harmonic (SH) component into axisymmetric χ^2 solitons is considered in the 2D system with the quadratic nonlinearity. The spontaneous conversion is driven by the parametric instability of the SH wave. The input in the form of the AW vortex is considered too. As a result, one, two, or three stable solitons emerge in a well-defined form, unlike the recently studied 1D setting, where the picture is obscured by radiation jets. Shares of the total power captured by the emerging solitons and conversion efficiency are found as functions of parameters of the AW input.

Intrinsic structure of waves may steer their propagation along curved trajectories, a well-known example being Airy waves (AWs) in linear media [1]-[4]. Realizations of AWs have been predicted and demonstrated in optics [3]-[9], plasmonics [10]-[12], electron beams [13], and gas discharge [14]. In linear media, the propagation of two-dimensional (2D) factorized AWs has been demonstrated too [1, 3, 4, 15, 16].

Considerable work has been done on the dynamics of AWs in media with cubic [17]-[22] and quadratic ($\chi^{(2)}$) [23]-[24] nonlinearities, including generation of solitons by AWs, and the 2D propagation in a $\chi^{(2)}$ medium [25]. Most works dealing with the $\chi^{(2)}$ nonlinearity addressed the *upconversion* scenario, i.e., the AW was launched in the fundamental-frequency (FF) component, generating the second-harmonic (SH) wave [26]-[28]. The *downconversion* of the 1D truncated AW launched in the SH, which spontaneously generates the FF component due to the parametric instability of the SH wave, was recently considered in Ref. [29]. The spontaneous downconversion, initiated by random perturbations amplified by the parametric instability [30, 31], produces sets of one, two, or three solitons alternating with irregular radiation “jets”. The generation of the solitons from the SH AW establishes the direct dynamical link between two distinct types of *eigenmodes* in the quadratic medium, *viz.*, the single-color AWs and two-color solitons.

The objective of the present work, suggested by the stability of fundamental 2D $\chi^{(2)}$ solitons [26]-[28] (the first reported $\chi^{(2)}$ solitons were two-dimensional [32]), is to establish such a link in 2D, via the spontaneous downconversion of two-dimensional AWs. The results are essentially “cleaner” than in the 1D case, i.e., emerging solitons are well pronounced, with no conspicuous radiation features or irregularities obscuring the picture. We also consider the downconversion of the input in the form of an AW vortex, which is another single-color eigenmode in 2D. In accordance with the fact that $\chi^{(2)}$ vortex solitons are unstable [33]-[35], it is found that such an input generates solely fundamental solitons.

The 2D spatial-domain evolution of the FF and SH wave amplitudes, u and w , is governed by well-known scaled equations [26]-[28]:

$$iu_z + (1/2)\nabla^2 u + u^*w = 0, \quad (1)$$

$$2iw_z - qw + (1/2)\nabla^2 w + u^2/2 = 0, \quad (2)$$

where z is the propagation distance, (x, y) transverse coordinates, ∇ the respective gradient, and the mismatch parameter may be scaled to three values: $q = -1, 0, +1$. The system

conserves the total power, vectorial momentum, and angular momentum (as well as the Hamiltonian):

$$P = \int \int (|u|^2 + 4|w|^2) dx dy, \quad (3)$$

$$\mathbf{M} = i \int \int [(u \nabla u^* + 2w \nabla w^*) - \text{c.c.}] dx dy, \quad (4)$$

$$\begin{aligned} \Omega = \frac{i}{2} \int \int \left\{ \left[u \left(x \frac{\partial}{\partial y} - y \frac{\partial}{\partial x} \right) u^* \right. \right. \\ \left. \left. + 2w \left(x \frac{\partial}{\partial y} - y \frac{\partial}{\partial x} \right) w^* \right] - \text{c.c.} \right\} dx dy, \end{aligned} \quad (5)$$

where c.c. stands for the complex-conjugate expression.

In the absence of the FF component, exact 2D eigenmodes are generated by the SH input in the form of factorized truncated AWs,

$$\begin{aligned} w(x, y, z = 0) &= W_0 \text{Ai}(\alpha x) \text{Ai}(\alpha y) e^{(\alpha/A)(x+y)} \\ &\equiv \text{AA}(x, y), \quad v(x, y, z = 0) = 0. \end{aligned} \quad (6)$$

where Ai is the Airy function, with W_0 and $1/\alpha$ determining the amplitude and spatial scale of the wave, whose total power is made finite by means of the truncation parameter, A [3]:

$$P = W_0^2 (8\pi\alpha^2)^{-1} A \exp[(4/3) A^{-3}]. \quad (7)$$

More general solutions may be produced by anisotropic inputs, with $\text{Ai}(\alpha y)$ in Eq. (6) replaced by $\text{Ai}(\beta y)$, $\beta \neq \alpha$.

Fundamental solutions of Eqs. (1) and (2) are 2D isotropic solitons, whose existence and stability for large $q > 0$ can be easily explained by means of the cascading limit [26]: in this case, a solution to Eq. (2) is approximated, at the first two orders, by $w = [(2q)^{-1} + (2q)^{-2} \nabla^2] (u^2)$. The substitution of this in Eq. (1) leads to a generalized nonlinear Schrödinger (NLS) equation,

$$iu_z + (1/2) \nabla^2 u + (2q)^{-1} |u|^2 u + (2q)^{-2} u^* \nabla^2 (u^2) = 0. \quad (8)$$

The last term here, which corresponds to term $\delta \mathcal{H} = (8q^2)^{-1} |\nabla(u^2)|^2$ in the Hamiltonian density, is similar to, but different from, the one which accounts for a finite interaction radius in the Gross-Pitaevskii equation for atomic Bose-Einstein condensates, *viz.*, $u \nabla^2 (|u|^2)$ [36].

A usual estimate [37] demonstrates that this term stabilizes 2D NLS solitons by arresting their collapse. It is shown below that the AW structure of the input, driving self-stretching of the field, prevents approaching the quasi-collapse in the $\chi^{(2)}$ system, and thus facilitates the creation of one or several solitons (a similar trend was reported in the cubic NLS equation [22]).

Results produced by systematic simulations of Eqs. (1) and (2) with initial conditions given by Eq. (6) with the FF component seeded by a small random perturbation with amplitude ~ 0.001 , are presented below for $q = 0$ and $q = +1$. The outcome does not depend on a particular realization of the random seed, which is explained by the fact that the system selects an eigenmode of the parametric instability from the random perturbation. In agreement with Eq. (8), solitons were not found at $q = -1$. The results are reported for $A \leq 20$, the respective FWHM width of the input in the x and y directions being ≤ 30 ; otherwise, the necessary integration domain is too large, and the respective spatial area of the experimental realization may also be too large.

The results for $q = 0$ are summarized in Fig. 1, which shows the number of solitons (none, one, or two) generated by the AW input, in the space of its parameters, (A, α, P) . The full diagram in the 3D parameter space looking cumbersome, Figs. 1(a,b) display its typical 2D slice projected onto the (A, α) and (A, P) planes. Naturally, the number of the solitons increases with P in Fig. 1(b). At $A \geq 10$, the results are simple in terms of α : two, one, and no solitons are generated, respectively, at $\alpha < 0.075$, $0.075 < \alpha < 0.17$, and $\alpha > 0.17$ in Fig. 1(a). Three solitons can be generated at very small α (this case is not shown in Fig. 1). In particular, three solitons with nearly equal powers, each carrying share $\simeq 0.12$ of the total input power (7), cf. Fig. 5 below, are generated by the input with $W_0 = 0.39$, $\alpha = 0.05$, $A = 5$.

Typical examples of the generation of a single soliton and two solitons are displayed in Figs. 2 and 3, respectively. In particular, the single soliton emerging in Fig. 2 traps the share of the initial total power (3) which is 0.251, the rest being spent on the generation of small-amplitude radiation (see also Fig. 5 below). For two solitons in Fig. 3, respective shares of the initial total power are 0.200 and 0.376. The figures display self-trapping of the originally diffuse fields, via transient oscillations, into quasi-stationary 2D solitons. Trajectories of the emerging solitons are clearly seen too. Note that, when the single soliton is generated, it moves in the same direction in which the self-bending AW, initiated by input (6), would

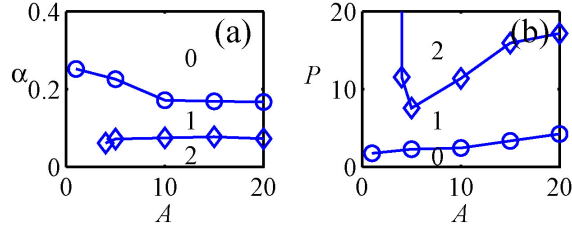


FIG. 1: (a,b): Projections of a typical slice of the diagram in the parameter space (A, α, P) onto planes (A, α) and (A, P) , showing the number of solitons (0, 1, or 2) generated by input (6) through the downconversion, in the system with $q = 0$.

move as the eigenmode of the linear SH equation. On the other hand, in Fig. 3 two solitons move in opposite directions, although the self-bending direction determined by the AW input remains dominant. It was checked that the simulations keep zero value of total momentum (4), in accordance with the fact that it is zero for input (6). The momentum of the moving solitons is compensated by recoil absorbed by the small-amplitude radiation.

As mentioned above, in the case of $q = 0$ in Eq. (2), the generation of three solitons by the AW input (6) requires very small values of α and, accordingly, a very broad simulation domain. The creation of multiple solitons is facilitated by taking $q = +1$, as shown in Fig. 4, where an additional weak soliton appears between two stronger ones. In this case, two emerging solitons move in the direction determined by the AW input, while the third (left) soliton moves backwards.

Unlike the 1D setting considered in Ref. [29], where relatively strong radiation “jets” were generated, in addition to solitons, making the overall picture rather messy, in the 2D system the radiation field does not form conspicuous features, allowing the solitons to emerge in a clean form, as seen in Fig. 5, where rhombus data points show the relative intensity of the FF radiation field outside of the soliton’s cores. The result is less clean in the case when two solitons are created, as the radiation field has a higher amplitude between them.

An essential characteristic of the emerging set of solitons is the share of total power (3) carried away by each one. For the cases when one or two solitons are generated, the corresponding results are summarized in Fig. 5 (in the region shown in the figure, three solitons do not emerge, but results for the three-soliton set created at $\alpha = 0.05$ are mentioned above, with each soliton’s power share close to 0.12). Naturally, the shares decrease with the increase of truncation parameter A in input (6), as the total power grows, roughly, $\sim A$,

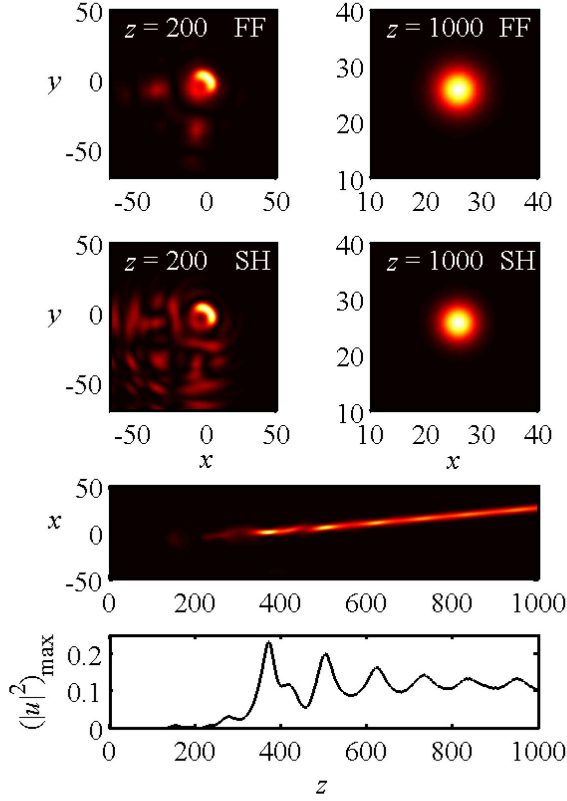


FIG. 2: A typical example of the generation of a single 2D soliton by input (6), with $W_0 = 0.3481$, $\alpha = 0.0857$, $A = 10$, and $q = 0$ in Eq. (2). The first and second rows display, respectively, distributions of the power density of the FF and SH components, u and w , in the transverse plane at the early stage of the evolution ($z = 200$), and at $z = 1000$, when the well-defined soliton is observed. The third and fourth rows: The evolution of the FF power-density profile in the projection onto plane (x, z) , and the peak power of the FF components vs. z , which illustrate the self-trapping of the soliton.

as per Eq. (7), while parameters of the emerging solitons weakly depend on A . The creation of the solitons is also characterized by the conversion efficiency, quantified in Fig. 5 by the share of the total power which is kept by the SH component of the wave field.

We also ran systematic simulations for the transformation of the Airy vortex, generated by input

$$w(x, y, z = 0) = (\partial/\partial x + i\partial/\partial y) AA(x, y), \quad (9)$$

where $AA(x, y)$ is the truncated factorized AW in Eq. (6). Angular momentum (5) of this waveform is $\Omega = 4 \int \int [(\partial AA/\partial x)^2 + (\partial AA/\partial y)^2] dx dy$. In the framework of the

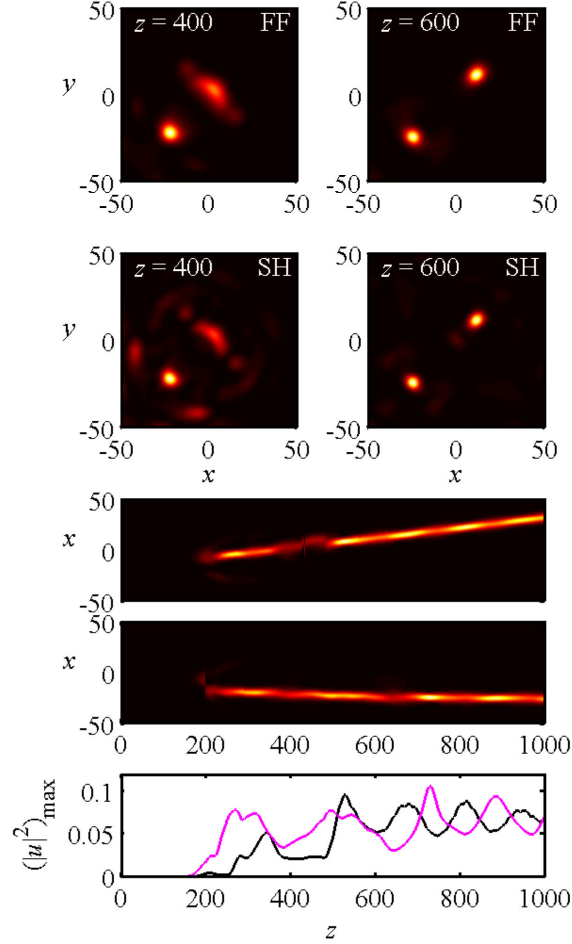


FIG. 3: The same as in Fig. 2, but for a typical example of the generation of two solitons, at $W_0 = 0.2984$, $\alpha = 0.05701$, $A = 10$, and $q = 0$. The third and fourth rows show, severally, the trajectories of the solitons. In the bottom row, magenta and black lines show the evolution of the peak powers of the FF component in the left and right solitons, respectively.

SH linear equation, this input gives rise to a solution produced by the action of operator $(\partial/\partial x + i\partial/\partial y)$ onto the AW.

A typical example of the vortex input and its evolution is displayed in Fig. 6. The mode quickly loses its vorticity and transforms into a single fundamental soliton, moving in the positive x direction. In the case shown in Fig. 6, the total input power (7) is 12.561, the emerging soliton carrying away its share ≈ 0.22 . The rest of the power is scattered in the form of small-amplitude radiation, which also absorbs the entire angular momentum of the initial vortex.

In conclusion, we have explored the scenario of the downconversion of AWs (Airy waves) in

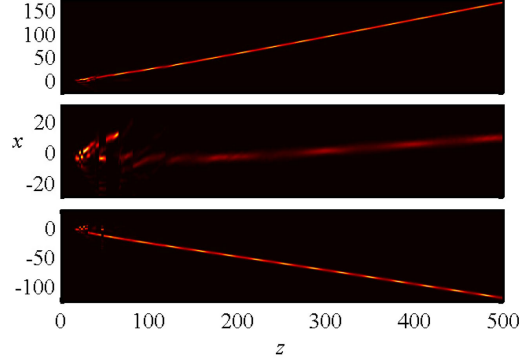


FIG. 4: Trajectories of three solitons generated with $W_0 = 3.183$, $\alpha = 0.1714$, $A = 10$, and $q = +1$ in Eq. (2).

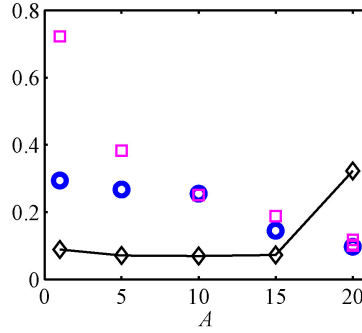


FIG. 5: The share of total power (3), trapped in the emerging solitons generated by Eqs. (1) and (2) with $q = 0$, is shown by squares as a function of truncation parameter A , while α is slightly varied to maintain constant FWHM = 20 of input (6). The double square at $A = 20$ labels the case when two solitons are created. The cleanness of the emerging solitons is quantified by rhombuses, which show the relative squared amplitude of the radiative component of the FF field, $(|u(x, y)|^2)_{\max}^{(\text{rad})} / (|u(x, y)|^2)_{\max}^{(\text{sol})}$, at $z = 1000$. Circles show the share of the total power (3) kept by the SH component.

the 2D $\chi^{(2)}$ medium, which is initiated by random perturbations amplified by the parametric instability of the AWs and Airy vortices in the SH component. The spontaneous downconversion generates one or more stable fundamental solitons in the “clean” form, unlike the 1D setting, where the picture is complicated by radiation jets. A challenging possibility is to extend the analysis to 3D, where the $\chi^{(2)}$ nonlinearity supports stable spatiotemporal solitons [38]–[40], that may be generated by the 3D instability of quasi-2D solitons [40–42].

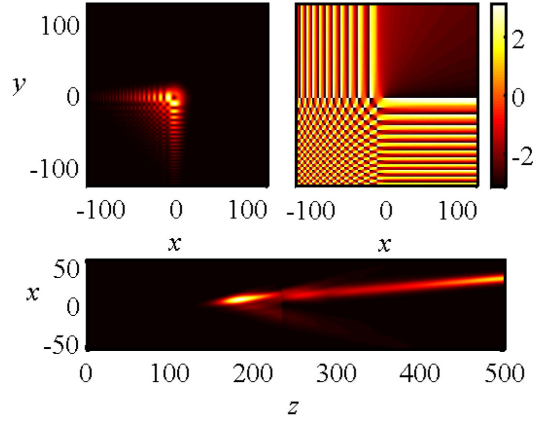


FIG. 6: Left and right top panels show the amplitude, $|w(x, y)|$, and phase distributions for the input in the form of the Airy vortex, given by Eq. (9) with $W_0 = 2.6452$, $\alpha = 0.171$, $A = 5$. The bottom panel displays the trajectory of the single fundamental soliton into which the vortex is converted.

Funding Information

Thailand Research Fund (TRF) (RSA5780061).

-
- [1] M. V. Berry and N. L. Balazs, *Am. J. Phys.* **47**, 264 (1979).
 - [2] M. V. Berry, *New J. Phys.* **7**, 129 (2005).
 - [3] G. A. Siviloglou and D. N. Christodoulides, *Opt. Lett.* **99**, 213901 (2007).
 - [4] G. A. Siviloglou, J. Broky, A. Dogariu, and D. N. Christodoulides, *Phys. Rev. Lett.* **99**, 213901 (2007).
 - [5] P. Polynkin, M. Kolesik, J. V. Moloney, G. A. Siviloglou, and D. N. Christodoulides, *Science* **324**, 229 (2009).
 - [6] P. Rose, F. Diebel, M. Boguslawski, and C. Denz, *Appl. Phys. Lett.* **102**, 101101 (2013).
 - [7] R. Driben, Y. Hu, Z. Chen, B. A. Malomed, and R. Morandotti, *Opt. Lett.* **38**, 2499 (2013).
 - [8] N. K. Efremidis, *Phys. Rev. A* **98**, 023841 (2014).
 - [9] Y. Zhang, M. R. Belić, L. Zhang, W. P. Zhong, D. Y. Zhu, R. M. Wang, and Y. P. Zhang, *Opt. Exp.* **23**, 10467 (2015).
 - [10] A. Minovich, A. E. Klein, N. Janunts, T. Pertsch, D. N. Neshev, and Y. S. Kivshar, *Phys.*

- Rev. Lett. **107**, 116802 (2011).
- [11] L. Li, T. Li, S. M. Wang, C. Zhang, and S. N. Zhu, Phys. Rev. Lett. **107**, 126804 (2011).
 - [12] I. Epstein and A. Arie, “Arbitrary Bending Plasmonic Light Waves”, Phys. Rev. Lett. **112**, 023903 (2014).
 - [13] N. Voloch-Bloch, Y. Lereah, Y. Lilach, A. Gover, and A. Arie, Nature **494**, 331 (2013).
 - [14] M. Clerici, Y. Hu, P. Lassonde, C. Milián, A. Couairon, D. N. Christodoulides, Z. Chen, L. Razzari, F. Vidal, F. Légaré, D. Faccio, R. Morandotti, Sci. Adv. **1**, e140011 (2015).
 - [15] D. G. Papazoglou, S. Suntsov, D. Abdollahpour, and S. Tsortsakis, Phys. Rev. A **81**, 061807 (2010).
 - [16] Z. Y. Ye, S. Liu, C. B. Lou, P. Zhang, Y. Hu, D. H. Song, J. L. Zhao, and Z. G. Chen, Opt. Lett. **36**, 3230 (2011).
 - [17] I. Kaminer, M. Segev, and D. N. Christodoulides, Phys. Rev. Lett. **106**, 213903 (2011).
 - [18] Y. Fattal, A. Rudnick, and D. M. Marom, Opt. Exp. **19**, 17298 (2011).
 - [19] Y. Hu, Z. Sun, D. Bongiovanni, D. Song, C. Lou, J. Xu, Z. Chen, and R. Morandotti, Opt. Lett. **37**, 3201 (2012).
 - [20] R. Driben, V. V. Konotop, and T. Meier, Opt. Lett. **39**, 5523 (2014).
 - [21] C. Ruiz-Jiménez, K. Z. Nóbrega, and M. A. Porras, Opt. Exp. **23**, 8918 (2015).
 - [22] R. Driben and T. Meier, Opt. Lett. **39**, 5539,(2014).
 - [23] T. Ellenbogen, N. Voloch-Bloch, A. Ganany-Padowicz, and A. Arie, Nature Phot. **3**, 395 (2009).
 - [24] I. Dolev, I. Kaminer, A. Shapira, M. Segev, and A. Arie, Phys. Rev. Lett. **108**, 113803 (2012).
 - [25] I. Dolev and A. Arie, Appl. Phys. Lett. **97**, 171102 (2010).
 - [26] G. I. Stegeman, D. J. Hagan, and L. Torner, Opt. Quant. Elect. **28**, 1691 (1996).
 - [27] C. Etrich, F. Lederer, B. A. Malomed, T. Peschel, and U. Peschel, Prog. Opt. **41**, 483 (2000).
 - [28] A. V. Buryak, P. Di Trapani, D. V. Skryabin, and S. Trillo, Phys. Rep. **370**, 63 (2002).
 - [29] T. Mayteevarunyoo and B. A. Malomed, Opt. Lett. **40**, 4947 (2015).
 - [30] G. Leo and G. Assanto, Opt. Lett. **22**, 1391(1997).
 - [31] M. T. G. Canva, R. A. Fuerst, S. Baboiu, and G. I. Stegeman, and G. Assanto, Opt. Lett. **22**, 1683(1997).
 - [32] W. E. Torruellas, Z. Wang, D. J. Hagan, E. W. Van Stryland, G. I. Stegeman, L. Torner, and C. R. Menyuk, Phys. Rev. Lett. **74**, 5036 (1995).

- [33] W. J. Firth and D. V. Skryabin, Phys. Rev. Lett. **79**, 2450 (1997).
- [34] L. Torner and D. V. Petrov, Electron. Lett. **33**, 608 (1997).
- [35] D. V. Petrov, L. Torner, J. Martorell, R. Vilaseca, J.P. Torres and C. Cojocaru, Opt. Lett. **23**, 1444 (1998).
- [36] J. J. García-Ripoll, V. V. Konotop, B. Malomed, and V. M. Pérez-García, Mathematics and Computers in Simulation **62**, 21 (2003).
- [37] G. Fibich, The Nonlinear Schrödinger Equation: Singular Solutions and Optical Collapse (Springer: Cham, 2015).
- [38] A. A. Kanashov and A. M. Rubenchik, Physica D **4**, 122 (1980).
- [39] B. A. Malomed, P. Drummond, H. He, A. Berntson, D. Anderson, and M. Lisak, Phys. Rev. E **56**, 4725 (1997).
- [40] B. A. Malomed, D. Mihalache, F. Wise, and L. Torner, J. Optics B: Quant. Semicl. Opt. **7**, R53 (2005).
- [41] X. Liu, K. Beckwitt, K, and F. Wise, Phys. Rev. Lett. **85**, 1871 (2000).
- [42] S. Minardi, J. Yu, G. Blasi, A. Varanavičius, G. Valiulis, A. Beržanskis, A. Piskarskas, and P. Di Trapani, Phys. Rev. Lett. **91**, 123901 (2003).